Nanosecond Dynamics of Poly(methyl methacrylate) Brushes in Solvents Studied by Fluorescence Depolarization Method

Hiroyuki Aoki,* Masafumi Kitamura, and Shinzaburo Ito

Department of Polymer Chemistry, Kyoto University, Nishikyo, Kyoto 615-8510, Japan

Received October 4, 2007
Revised Manuscript Received December 10, 2007

Introduction. Grafting of the polymer chain on a solid substrate is a common technique to modify the surface properties and has been widely used in various fields.[1−3] Recent development of the controlled polymerization technique enabled us to graft the polymer chain onto a solid surface with an extremely high chain density, so-called "polymer brush".[4,5] The high-density polymer brush shows different properties from the equivalent polymer film: for example, a glass transition temperature higher than a bulk state,[6−8] the strong resistance against the compression in the normal direction to the substrate,[8] and the reduction of the swelling capacity by a solvent.[9] The properties characteristic of the high-density polymer brush are attributed to the stretched conformation and the restricted motion of the brush chain. The fundamental process of the dynamics of the polymer brush chain is important for understanding the physical properties on the macroscopic scale. Whereas the dynamic properties of the polymer brush has been extensively studied by theoretical and numerical methods,[10−13] few experimental works have been reported because it is difficult to obtain the signal from the thin layer of the polymer brush tethered on a substrate due to the extremely small sample volume.[14−17] In this communication, we report the dynamics of poly(methyl methacrylate) (PMMA) brush investigated by the fluorescence depolarization method. We examined the temporal profile in the nanosecond time range of the anisotropy of the fluorescence signal from the dye-labeled PMMA brush, which corresponds to the second-order orientational autocorrelation function of the fluorescent moiety.[18−20] We examined the dynamics of the brush chain for the PMMA brush samples with different graft densities and discuss the effect of swelling solvents on the local chain dynamics.

Materials and Methods. The dye-labeled graft PMMA was prepared by the surface-initiated atom transfer radical copolymerization of methyl methacrylate (MMA) and perylenylmethyl methacrylate (PeMMA).[21,22] A clean quartz plate was immersed in a toluene solution of [2-(4-chlorosulfonylphenyl)-ethyl]trichlorosilane (CTCS) and phenethyltrichlorosilane (PhTCS) for 2 h. The concentration of the surface initiator on the substrate was adjusted by changing the feed ratio of CTCS and PhTCS. The substrate was then transferred into a mixed solution of MMA, PeMMA, CuBr, dinonylbipyridine, and *p*-toluenesulfonyl chloride (TsCl). The fraction of the perylene moiety was less than 0.005% to avoid the fluorescence depolarization due to the energy migration among the perylene molecules. The polymerization was carried out at 90 °C in vacuum. The sample was cleaned by Soxhlet extraction with THF to remove the linear polymer in solution generated from TsCl, which is called "free polymer." The weight- and number-average molecular weights, M_w and M_n, of the graft chain can be estimated from those of the free polymer,[23] which was determined by size exclusion chromatography calibrated with the PMMA standards. The thickness of the graft PMMA film was determined by atomic force microscopy (SPM-9500, Shimadzu or NanoWizard, JPK). A part of the polymer film in the dry state was scratched with a sharp needle to expose the substrate, and the thickness was defined as the height difference between the polymer and substrate surfaces. The graft density, σ, was evaluated from the thickness of the PMMA brush layer in the dry state and molecular weight. We prepared three PMMA brush samples, PMMA−L, PMMA−M, and PMMA−H, with different graft densities. The characterization of the brush samples is as follows: $M_n = 1.01 \times 10^5$; $M_w/M_n = 1.14$; $\sigma = 0.11$ chains nm^{-2} for PMMA−L, and $M_n = 1.08 \times 10^5$; $M_w/M_n = 1.19$; $\sigma = 0.37$ chains nm^{-2} for PMMA−M, and $M_n = 1.11 \times 10^5$; $M_w/M_n = 1.17$; $\sigma = 0.46$ chains nm^{-2} for PMMA−H.

The time-resolved fluorescence anisotropy was measured by the time-correlated single photon counting (TCSPC) method[18] under a home-built confocal microscope. The linearly polarized excitation pulse at 442 nm of the second harmonic of a Ti:sapphire laser (Tsunami, Spectra-Physics) was focused on the PMMA graft layer swollen in a solvent through a microscope objective (20×, 0.2 NA, Nikon). The fluorescence signal from the sample was collected by the same objective and input to a polarizing beam splitter to separate the polarization components, $I_{\|}$ and $I_{\perp}$, parallel and perpendicular to the polarization direction of the excitation light, respectively, and they were simultaneously detected by two photomultipliers (H8632, Hamamatsu Photonics). The photon signal was fed to TCSPC electronics (SPC-630, Becker & Hickl) to acquire the fluorescence decay curve for each channel. The full width at the half-maximum of the instrument response function was ca. 180 ps. The fluorescence anisotropy, $r(t)$, defined as the following equation:

$$r(t) = \frac{I_{\|}(t) - g\, I_{\perp}(t)}{I_{\|}(t) + 2g\, I_{\perp}(t)} \qquad (1)$$

Here g is the correction factor to compensate the difference of the detection sensitivity between the two photomultipliers. The measured anisotropy was fitted to a model function $r_{\mathrm{fit}}(t)$ consisting of the sum of two exponential functions by a nonlinear least-square method considering the convolution of the instrument response function. The mobility of the brush chain is discussed in terms of the correlation time, τ_c, defined as

$$\tau_c = \int_0^{\infty} r_{\mathrm{fit}}(t)/r_{\mathrm{fit}}(0)\, \mathrm{d}t \qquad (2)$$

Results and Discussion. Figure 1 shows the fluorescence anisotropy decay curves for the graft PMMA swollen in benzene and the free PMMA in benzene solutions. The time-resolved anisotropy showed multicomponent exponential decay, indicating that the local motion of a polymer chain should consist of the sum of various motional modes with different time scales; however, the experimental anisotropy could be well fitted to a double-exponential function practically. The free PMMA chain in the solution at a concentration of 0.33 g/mL showed the decay of fluorescence anisotropy with a correlation time of 9.9 ns

---

* Corresponding author: Telephone: +81-75-383-2613. Fax: +81-75-383-2617. E-mail: aoki@photo.polym.kyoto-u.ac.jp.

10.1021/ma7022149 CCC: $40.75

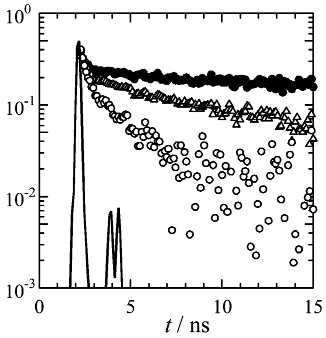

Figure 1. Fluorescence anisotropy decay curves for the PMMA brush swollen in benzene (filled circles) and the free PMMA chain in benzene solution at concentrations of 0.33 (triangles) and 2.9×10^{-3} g/mL (open circles). The graft density of the brush is 0.46 chains nm^{-2}. The solid curve indicates the instrument response function.

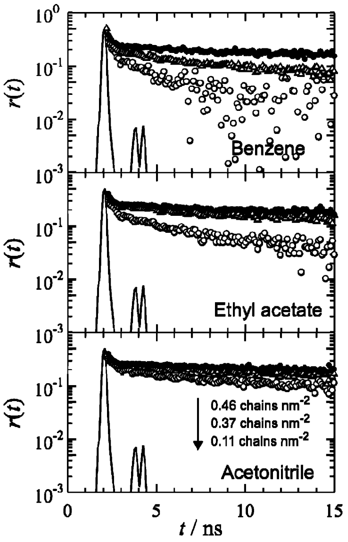

Figure 2. Fluorescence anisotropy decay curves for the PMMA brush swollen in benzene (top), ethyl acetate (middle), and acetonitrile (bottom). The filled circles, triangles, and open circles indicate the data for the brush sample with the graft densities of 0.46, 0.37, and 0.11 chains nm^{-2}, respectively. The solid curves indicate the instrument response function.

slower than that in the dilute solution ($\tau_c = 2.3$ ns). The motion of the polymer chains is suppressed by the interchain interaction at the concentration of 0.33 g/mL, which is larger than the overlap concentration c^*.[24] The concentration of 0.33 g/mL corresponds to the average polymer concentration in the PMMA brush layer with the graft density of 0.46 chains nm^{-2} (the averaged polymer concentration in the brush layer was estimated from its thickness in the dry and swollen states). Even at the same polymer concentration, the brush chain showed a large correlation time of 31 ns compared to the corresponding solution system. Such low mobility of the brush chain can be attributed to the effect of fixation of the chain end onto the solid substrate. For the linear polymer chain in solution, both chain ends show high mobility compared with the center segment in the main chain.[25] In the case of the polymer brush, one end is chemically bound to the substrate. Therefore, the segmental motion is greatly suppressed at the fixed end of the brush chain, resulting in a large correlation time compared to the free chain in solution.

The dynamics of PMMA brush chains is discussed in terms of the effect of graft density. Figure 2 shows the fluorescence anisotropy decay observed for the graft PMMA chain swollen in acetonitrile, ethyl acetate, and benzene. For each swelling solvent, the chain mobility is dependent on the graft density. The higher the graft density is, the slower the segmental mobility is. At the high graft density, the steric interaction between the brush chains results in the suppressed molecular motion.

Table 1. Chain Dimension in the Normal Direction to the Substrate Surface

sample	solvent	σ/chains nm^{-2}	L_e/nm	L_e/L_0
PMMA−L	acetonitrile	0.11	25	0.098
PMMA−L	benzene	0.11	130	0.51
PMMA−H	acetonitrile	0.46	161	0.58
PMMA−H	benzene	0.46	253	0.91

Now we discuss the solvent dependence of the dynamics of the PMMA brush. For the PMMA brush with $\sigma = 0.11$ chains nm^{-2}, the anisotropy decay curves (blue circles in Figure 2) clearly indicate that the mobility of the brush chain is high in a good solvent of benzene and low in a Θ solvent of acetonitrile. The correlation time in the swelling solvents of acetonitrile, ethyl acetate, and benzene is 15, 5.4, and 2.3 ns, respectively. The chain mobility is greatly dependent on the solvent quality: the better the solvent quality is, the faster the segmental motion of the brush chain is. Similar solvent dependence has been reported also for the dynamics of a polymer brush at a longer time scale of 10^{-6}−10^{-3} s.[16,17] This result indicates that the solvent dependence of the PMMA brush is similar to the solution system. The previous study showed that the local motion of the polymer chains in solution depends on the solvent quality.[26] The chain conformation in solution greatly affects the local motion of the polymer chain; the shrunken conformation in a poor solvent causes the steric interaction among the chain segments, resulting in the lowest mobility in acetonitrile and the highest in benzene. Similarly to the behavior of free polymer chain in solution, the PMMA brush chain takes a more expanded conformation in good solvents, resulting in the highest segmental mobility in benzene.

On the other hand, the PMMA brush with a high graft density showed solvent dependence different from the solution state. The brush with the high graft density of 0.46 chains nm^{-2} did not show significant solvent dependence as illustrated in Figure 2. The correlation time was 39, 32, and 29 ns for the brush swollen in acetonitrile, ethyl acetate, and benzene, respectively. As mentioned above, the nanosecond dynamics in solution depends on the chain conformation determined by the solvent quality. Also for the PMMA brush, the chain conformation would be a dominant factor of the chain mobility.

The chain dimension in the normal direction to the substrate was experimentally evaluated as the thickness of the brush layer immersed in a solvent, which can be observed by atomic force microscopy in a liquid condition.[27] Table 1 summarizes the chain dimension normal to the substrate as the observed thickness in the equilibrium swelling state (L_e) and the ratio of L_e to the contour length of the brush chain (L_0). The thickness of the PMMA brush with $\sigma = 0.46$ chains nm^{-2} is 161 nm in acetonitrile, which is corresponding to approximately 60% of the contour length of the brush chain. In the good solvent of benzene, the thickness and L_e/L_0 are 253 nm and 90%, respectively. This indicates that the brush chain takes an extremely stretched conformation in the normal direction to the substrate surface at the high graft density. Such a stretched conformation of the brush chain results from the strong repulsive interaction among the brush chains since the PMMA chain is densely packed on the substrate. It should be noted that the difference between the chain dimensions in both solvents is only 36% for the PMMA brush with the high graft density. For the high-density brush, the strong repulsive interaction between the neighboring chains makes the chain conformation stretched even in the poor solvent. Therefore, the chain dynamics of the high-

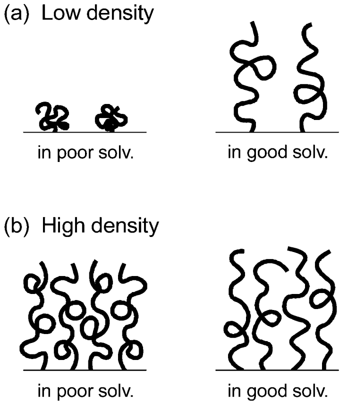

Figure 3. Schematic drawing of the PMMA brush chain with the low (a) and high graft density (b). The left- and right-hand sides of each image illustrate the brush chains in poor and good solvents, respectively.

density PMMA brush does not show significant solvent dependence. In the case of the low-density brush, the interaction among the brush chains is relatively weak and the brush chain can easily change its conformation, resulting in a sensitive response of the chain conformation to the solvent quality. Consequently, the chain dimensions in benzene and acetonitrile differ by more than 5 times in Table 1. The solvent dependence of the chain conformation is schematically depicted in Figure 3. As mentioned above, the chain dimension in the swollen state in solvents is a dominant factor to determine the segmental mobility of the PMMA brush chain. Because of the similar chain conformations in the poor and good solvents, the micro-Brownian motion of the high-density PMMA brush chain is not affected by the solvent quality, whereas the low-density brush chain changes its mobility dependent on the solvent. We discussed the chain dynamics in terms of the correlation time, τ_c, which correspond to the averaged relaxation time of the two time constants for a double-exponential decay fitted to the fluorescence anisotropy data. As mentioned above, the fluorescence anisotropy showed multiexponential decay. The concentration of the chain segment is the highest at the substrate and gradually decreases with the distance from the substrate.[28,29] Since we used the PMMA brush labeled along the whole chain contour in the current study, the segment density profile result in the multicomponent exponential decay of the fluorescence anisotropy. The fast and slow decay components correspond to the motion of the segments near the free and fixed ends of the brush chain, respectively. However, the assignment of each decay component is not clear at present. Now we are studying the physical meaning of the multicomponent exponential decay using the PMMA brush sample labeled at a selective position along the chain contour, and the further discussion will be published elsewhere.

Summary. The nanosecond chain dynamics of PMMA brushes was examined by the time-resolved fluorescence depolarization technique in the swollen condition in poor and good solvents. The low mobility of the brush chain compared to the free chain in a solution can be attributed to the effect of the fixed chain end on the solid substrate. The chain mobility of the PMMA brush with a high graft density does not show significant dependence on the solvent quality, whereas the dynamics of the low-density brush chain is sensitively affected by the swelling solvent. The chain dimension measurement in the swollen state revealed that such a unique behavior of the dynamics for the high-density PMMA brush results from the expanded conformation unaltered by the solvent quality due to the strong repulsive interaction among the brush chains.

Acknowledgment. We would like to thank Prof. Y. Tsujii and Prof. T. Fukuda, Institute for Chemical Research, Kyoto University, for the AFM measurement in the liquid conditions. This work was supported by a Grant-in-Aid from Japan Society for the Promotion of Science (JSPS) and a Grant-in-Aid for Scientific Research in Priority Area "Molecular Nano Dynamics" from Ministry of Education, Culture, Sports, Science, and Technology (MEXT), Japan. The Innovative Techno-Hub for Integrated Medical Bioimaging Project of the Special Coordination Funds for Promoting Science and Technology from MEXT is also acknowledged.

References and Notes

(1) Uyama, Y.; Kato, K.; Ikada, Y. *Adv. Polym. Sci.* **1998**, *137*, 1−39.
(2) Kato, K.; Uchida, E.; Kang, E. T.; Uyama, Y.; Ikada, Y. *Prog. Polym. Sci.* **2003**, *28*, 209−259.
(3) Senaratne, W.; Andruzzi, L.; Ober, C. K. *Biomacromolecules* **2005**, *6*, 2427−2448.
(4) Pyun, J.; Kowalewski, T.; Matyjaszewski, K. *Macromol. Rapid Commun.* **2003**, *24*, 1043−1059.
(5) Tsujii, Y.; Ohno, K.; Yamamoto, S.; Goto, A.; Fukuda, T. *Adv. Polym. Sci.* **2006**, *197*, 1−45.
(6) Tate, R. S.; Fryer, D. S.; Pasqualini, S.; Montague, M. F.; de Pablo, J. J.; Nealey, P. F. *J. Chem. Phys.* **2001**, *115*, 9982−9990.
(7) Yamamoto, S.; Tsujii, Y.; Fukuda, T. *Macromolecules* **2002**, *35*, 6077−6079.
(8) Urayama, K.; Yamamoto, S.; Tsujii, Y.; Fukuda, T.; Neher, D. *Macromolecules* **2002**, *35*, 9459−9465.
(9) Devaux, C.; Cousin, F.; Beyou, E.; Chapel, J. P. *Macromolecules* **2005**, *38*, 4296−4300.
(10) Lai, P. Y.; Binder, K. *J. Chem. Phys.* **1992**, *97*, 586−595.
(11) Wittmer, J.; Johner, A.; Joanny, J. F.; Binder, K. *J. Chem. Phys.* **1994**, *101*, 4379−4390.
(12) Semenov, A. N. *Langmuir* **1995**, *11*, 3560−3564.
(13) Semenov, A. N.; Anastasiadis, S. H. *Macromolecules* **2000**, *33*, 613−623.
(14) Fytas, G.; Anastasiadis, S. H.; Seghrouchni, R.; Vlassopoulos, D.; Li, J. B.; Factor, B. J.; Theobald, W.; Toprakcioglu, C. *Science* **1996**, *274*, 2041−2044.
(15) Jeon, S.; Bae, S. C.; Granick, S. *Macromolecules* **2001**, *34*, 8401−8404.
(16) Yakubov, G. E.; Loppinet, B.; Zhang, H.; Ruhe, J.; Sigel, R.; Fytas, G. *Phys. Rev. Lett.* **2004**, *92*, 4.
(17) Michailidou, V. N.; Loppinet, B.; Vo, D. C.; Prucker, O.; Ruhe, J.; Fytas, G. *J. Polym. Sci., Part B: Polym. Phys.* **2006**, *44*, 3590−3597.
(18) O'Conner, D. V.; Phillips, D. *Time-Correlated Single Photon Counting*; Academic Press: London, 1984.
(19) Aoki, H.; Horinaka, J.; Ito, S.; Yamamoto, M. *Polym. Bull. (Berlin)* **1997**, *37*, 109−116.
(20) Aoki, H.; Horinaka, J.; Ito, S.; Yamamoto, M.; Katayama, H.; Kamigaito, M.; Sawamoto, M. *Polym. J.* **2001**, *33*, 464−468.
(21) Ejaz, M.; Yamamoto, S.; Ohno, K.; Tsujii, Y.; Fukuda, T. *Macromolecules* **1998**, *31*, 5934−5936.
(22) Aoki, H.; Tanaka, S.; Ito, S.; Yamamoto, M. *Macromolecules* **2000**, *33*, 9650−9656.
(23) Ejaz, M.; Tsujii, Y.; Fukuda, T. *Polymer* **2001**, *42*, 6811−6815.
(24) The overlap concentration is estimated to be 0.12 g/mL in a Θ condition from the radius of gyration reported in the literature: Arai et al. *Macromolecules* **1996**, *29*, 2309. For the benzene solution, c^* should be smaller than 0.12 g/mL, because the PMMA chain takes an expanded conformation in the good solvent.
(25) Horinaka, J.; Maruta, M.; Ito, S.; Yamamoto, M. *Macromolecules* **1999**, *32*, 1134−1139.
(26) Horinaka, J.; Ono, K.; Yamamoto, M. *Polym. J.* **1995**, *27*, 429.
(27) Yamamoto, S.; Ejaz, M.; Tsujii, Y.; Matsumoto, M.; Fukuda, T. *Macromolecules* **2000**, *33*, 5602−5607.
(28) Habicht, J.; Schmidt, M.; Ruhe, J.; Johannsmann, D. *Langmuir* **1999**, *15*, 2460−2465.
(29) Karim, A.; Satija, S. K.; Douglas, J. F.; Ankner, J. F.; Fetters, L. J. *Phys. Rev. Lett.* **1994**, *73*, 3407−3410.

MA7022149